International Journal of Modern Physics B
Vol. 17, Nos. 8 & 9 (2003) 1141–1146
© World Scientific Publishing Company

World Scientific
www.worldscientific.com

EVALUATION OF THIN-FILM RESIDUAL STRESS USING NANO-INDENTATION COMBINED WITH AN ATOMIC FORCE MICROSCOPE

YUN HEE LEE* and DONGIL KWON

School of Materials Science and Engineering, Seoul National University, Seoul, 151-742, Korea

JAE IL JANG

Frontics, Inc., Research Institute of Advanced Materials, Seoul National University, Seoul, 151-742, Korea

Received 4 July 2002
Revised 7 November 2002

Thin-film stress changes the shape of nanoindentation loading curve. The change in the indentation load is treated as the effect of the residual stress on the indenting deformation. A residual-stress-induced normal load is defined as a multiple of contact area and plastic deformation-sensitive deviator stress component extracted from the equi-biaxial thin-film stress. A final equation for the residual stress is derived from the residual-stress-induced normal load by considering an integration along a depth-controlled stress-relaxation route. This proposed model is applied to the analyses of the nanoindentation curves for diamond-like carbon thin films. The residual stresses from the nanoindentation analyses were consistent with the values obtained by the conventional curvature method.

1. Introduction

Residual stress changes fatigue strength[1] and wear resistance, and also causes failure of thin film by cracking or interfacial delamination.[2] Curvature technique has been used as a thin film stress-measuring method by the merits of non-contact and in-situ execution.[3] However, it has the drawback of producing an averaged stress over a long scanning area.

Local nanoindentation technique was therefore proposed as a new nondestructive stress-characterizing method for thin film.[4,5] It has been applied to the evaluation of hardness and elastic modulus of thin film by analyzing the unloading curve in Fig. 1. Contact depth h_c was calculated from Eq. (1) for a three-sided pyramidal indenter[6] (h_i means an intercept depth):

$$h_C = h - 0.72(h - h_i) = h - 0.72\left(\frac{L}{S}\right). \tag{1}$$

Contact area A_c is converted from the contact depth by considering the geometry of the indenter. Reduced modulus E_r, involving the elastic properties of thin film and indenter,

* E-mail: uni44@mmrl.snu.ac.kr

is expressed[6] in Eq. (2) using the unloading slope S in Fig. 1 and the contact area:

$$E_r = \frac{\sqrt{\pi}S}{2\sqrt{A_C}} = \frac{\sqrt{\pi}L}{2(h-h_i)\sqrt{A_C}}. \tag{2}$$

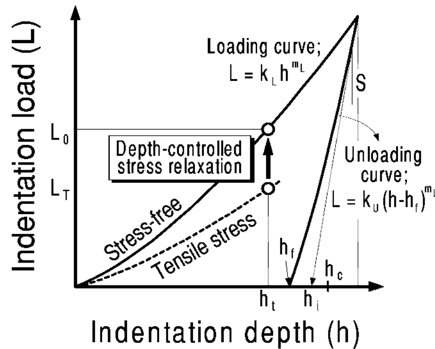

Fig. 1. Analysis of the contact depth from the unloading curve[6] and the shape change in the indentation loading curve by the existence of the tensile residual stress.[4,5]

The indentation loading curve altered by the equi-biaxial tensile stress is shown as the dotted line in Fig. 1. The change in the indentation curve due to the externally applied stress was empirically investigated through the precise observation of the indentation marks in the previous study.[4] In this study, we try to model the residual stress effect on the shape of the indentation curve theoretically. Indentation load L_T for the tensile stressed state increases to L_0 by stress relaxation at a constant indentation depth h_t.[4,5] A residual stress-analyzing equation is derived by considering stress interaction and relaxation from the viewpoint of plastic deformation. This model is used to assess the residual stresses in diamond-like carbon (DLC) thin films. The DLC thin films with special functions have been fabricated in industry for various usages.[7]

2. Theoretical Model

The effect of residual stress on the indenting deformation is considered from a plastic deformation-sensitive deviator stress. The equi-biaxial thin-film stress is separated as the mean stress and the shear deviator parts in Eq. (3). σ_{33}^{D} in the deviator stress part, parallel to the indentation axis, directly affects the indentation load. The effect of the residual stress on the indentation deformation is defined as a residual-stress-induced normal load L_{res}. And, L_{res} is formulated as $-2\sigma_{res}A_C/3$ $(=\sigma_{33}^{D}A_C)$.

$$\underbrace{\begin{pmatrix} \sigma_{res} & 0 & 0 \\ 0 & \sigma_{res} & 0 \\ 0 & 0 & 0 \end{pmatrix}}_{\text{Thin film stress}} = \underbrace{\begin{pmatrix} \frac{2}{3}\sigma_{res} & 0 & 0 \\ 0 & \frac{2}{3}\sigma_{res} & 0 \\ 0 & 0 & \frac{2}{3}\sigma_{res} \end{pmatrix}}_{\text{Mean stress part } (\sigma^{M})} + \underbrace{\begin{pmatrix} \frac{1}{3}\sigma_{res} & 0 & 0 \\ 0 & \frac{1}{3}\sigma_{res} & 0 \\ 0 & 0 & -\frac{2}{3}\sigma_{res} \end{pmatrix}}_{\text{Deviator stress part } (\sigma^{D})} . \quad (3)$$

Therefore, the thin-film stress can be evaluated by analyses of L_{res} from the loading curve and A_c from the unloading curve. However, the modeled contact area in Fig. 2, assuming the residual stress-independent intrinsic hardness and the stress-sensitive shape change in the indentation loading curve,[4,5] is not constant but varies with the stress state.

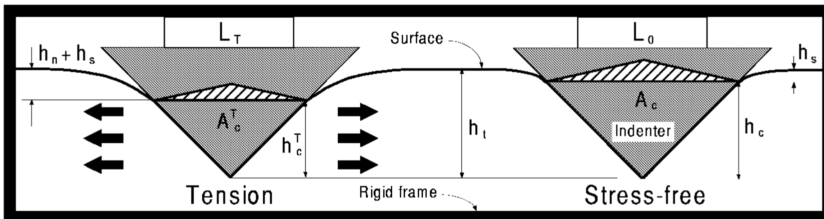

Fig. 2. Changes in the contact morphology during a depth-controlled stress relaxation. The contact area and the indentation load increase by the tensile stress relaxation.

The change in the contact morphology during a depth-controlled residual stress relaxation is considered in Fig. 2. A rebounding force occurs by removing the tensile residual stress (solid arrows in Fig. 2). The force pushes the indenter out from the surface as the tensile stress relaxes to the stress-free state at the fixed indentation depth h_t.[5] However, the force is constrained by the rigid frame to manifest itself as the increases of the indentation load ($L_T \rightarrow L_0$) and the contact area ($A_C^T \rightarrow A_C$). This continuous stress relaxation is expressed as an integration method in Eq. (4) using the definition of L_{res}:

$$L_0 = L_T + L_{res} = L_T - \frac{2}{3}\int_{L_T}^{L_0} d(\sigma \cdot A_C) . \quad (4)$$

The changes in the contact area (A_c) and the in-plane stress (σ) in the thin film during the stress relaxation should be expressed as equations of the indentation load to solve Eq. (4). Linear relaxation of stress is assumed and the contact area is fitted as an equation of the third degree in the indentation load. The equation for thin-film stress in Eq. (5) is derived from Eq. (4) using the equations of the contact area and the stress variation. Ω is given by

$$R_3 L_T^4 + (R_2 - R_3 L_0) L_T^3 + (R_1 - R_2 L_0) L_T^2 + (R_0 - R_1 L_0) L_T - R_0 L_0 .$$

R_0 to R_3 are fitting constants in the polynomial equation of the contact area.

$$\sigma_{res} = \frac{3}{2}\frac{L_{res}^2}{\Omega}. \quad (5)$$

3. Experimental Procedure

Two kinds of 0.4 μm and 0.6 μm thick DLC thin films were deposited on Si substrates using radio-frequency plasma-assisted chemical vapor deposition (R.F.-PACVD) with C_6H_6 source gas. Averaged surface roughnesses measured using an atomic force microscope (AFM) were 8.6±3.1nm and 1.8±1.3nm for the 0.4 μm and 0.6 μm thick DLC films, respectively. The deposited thin films were prepared as nanoindentation specimens of size 5 mm×5 mm. Free-standing films (stress-free state) for comparison with the as-deposited films (residually stressed state) were fabricated by wet-etching of the Si substrate in 60% HNO_3 + 30% HF + 10% CH_3COOH solution.[5] The free-standing films were rinsed with ethylalcohol, placed on Si bases without adhesive and indented.

The nanoindentation was performed using the Triboscope™ of Hysitron, Inc. Smooth testing area (roughness < 4.0nm) was selected by AFM pre-scanning before indentation. Maximum indentation depth was determined to be less than 1/10 of the film thickness, thus excluding the effect of the substrate deformation. The indentation loads satisfying this indentation depth condition were 1000 μN and 2000 μN for the 0.4 μm and 0.6 μm thick DLC films, respectively. Testing was repeated 10 times for each film with a loading speed of 250 μN/s using the Berkovich indenter. A representative indentation curve for each stress state was selected from the 10 superposed indentation curves and analyzed. The thin-film stress evaluated from this model was compared with the average value measured from the curvature method.

4. Results and Discussion

The representative indentation curves from the as-deposited and the free-standing DLC films are superposed in Fig. 3. The compressive stress sign is detected from the leftwards shift of the indentation loading curve for the as-deposited film comparing with that for the freestanding film. The residual-stress-induced normal load is the difference of the indentation loads for the as-deposited and the free-standing films at a selected indentation depth. The contact areas corresponding to various indentation load steps must be analyzed to express A_c as an equation of the indentation load L. The contact depth for the final unloading curve is calculated from Eq. (1) for each freestanding film in Fig. 3. The reduced modulus of the DLC film/diamond indenter couple was predetermined from Eq. (2) and was taken as an invariant intrinsic value regardless of the change in the indentation load.

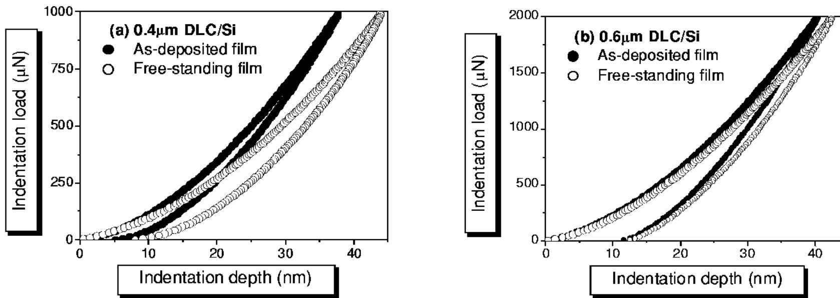

Fig. 3. Shape change in the indentation load-depth curves for (a) 0.4 μm and (b) 0.6 μm thick DLC thin films arising from the residual stress.

A calculated reduced modulus from Eq. (2) at a certain indentation load was compared with the predetermined intrinsic value. Contact depth at each selected load was determined from an indentation depth yielding the same value with the predetermined intrinsic reduced modulus. The contact area converted from the predicted contact depth for the Berkovich indenter is expressed as the function of the indentation load in Table 1.

Table 1. Predicted contact properties at each selected load and experimentally fitted equation for the contact area with the indentation load.

0.4μm-thick DLC free-standing film			0.6μm-thick DLC free-standing film		
Indentation load (μN)	Contact depth (nm)	Contact area (nm^2)	Indentation load (μN)	Contact depth (nm)	Contact area (nm^2)
800	27.2	256976.1	1950	28.0	83985.7
600	22.5	194585.5	1550	23.3	61346.6
400	17.0	127813.0	1150	18.2	40775.6
200	10.3	58445.0	750	12.9	24285.5
$A_C = -7.726\times10^{-5}L^3 + 0.098L^2 + 295.738L - 1960.460$			$A_C = -5.662\times10^{-6}L^3 + 0.032L^2 - 4.727L + 11994.863$		

Residual stresses in DLC films were evaluated by inputting the analyzed data into Eq. (5) and were compared with the results from the curvature method. The validity of the nanoindentation model was proved from the consistency in the residual stresses yielded by the two methods, as shown in Table 2.

Table 2. Residual stresses analyzed via the nanoindentation technique agree well with average stresses derived from the curvature method for the two DLC thin films.

Thin film	Nanoindentation technique (stress-relaxation model)	Curvature method
0.4 μm DLC/Si	−1.08±0.05 GPa	−0.98±0.07 GPa
0.6 μm DLC/Si	−3.04±0.16 GPa	−3.80±0.50 GPa

However, the average stress measured from the curvature method exceeded the analyzed value from the proposed model by 25% for the 0.6 μm-thick DLC film. This

discrepancy is explained as two causes. The first is plastic deformation of silicon substrate by high residual stress in the DLC film. A flow stress roughly estimated from the hardness of the single-crystalline Si[8] was 3.3GPa. The measured stress from the curvature method exceeded the predicted flow stress and yielding may have occurred in the Si substrate. In this case, plastic deformation would be added to the residual-stress-induced elastic bending deformation of the substrate, thus overestimating the average stress measured from the apparent curvature. Residual stress in the thin film is also reduced by the yield of the substrate. The other reason for the discrepancy is the size difference of the testing areas of the two techniques. The stress measurement area (20mm × 20mm) of the curvature method is larger than that (5mm × 5mm) of the nanoindentation technique. We therefore believe that the local variation of residual stress can be neglected in the curvature method.

5. Conclusions

This study proposes a residual stress-analysis model using the nanoindentation technique. The model was applied to the characterization of DLC films and the detailed conclusions below were obtained.

1) The deviator stress was separated from the equi-biaxial thin-film stress to explain the stress effect on the indenting plastic deformation. And, the stress-analysis equation was derived from an integral expression of the depth-controlled stress relaxation.
2) The residual stresses evaluated from the proposed model were –1.08±0.05 GPa and –3.04±0.16GPa for the 0.4 μm and 0.6 μm thick DLC films, respectively. The average stresses measured from the curvature method were comparable: –0.98±0.07 GPa and –3.80±0.50 GPa for the two thin films.
3) The stress overestimation for the 0.6 μm DLC film from the curvature method was explained by the plastic deformation of Si substrate, which increases the apparent bending curvature of the substrate and decreases the residual stress in the thin film.

Acknowledgments

This work was supported by the Korean Ministry of Science and Technology as a part of the National Research Laboratory Program.

References

1. C.-M. Suh, B.-W. Hwang and K.-R. Kim, *Int. J. Mod. Phys. B*, **16**, 181 (2002).
2. W. D. Nix, *Metall. Trans. A*, **20A**, 2217 (1989).
3. P. A. Flinn, *Mater. Res. Soc. Symp. Proc.*, **130**, 41 (1989).
4. T. Y. Tsui, W. C. Oliver and G. M. Pharr, *J. Mater. Res.*, **11**, 752 (1996).
5. Y.-H. Lee and D. Kwon, *J. Mater. Res.*, **17**, 901 (2002).
6. W. C. Oliver and G. M. Pharr, *J. Mater. Res.*, **7**, 1564 (1992).
7. P. R. Vinod, H. Kakiuchi, T. Terai, A. N. Itakura and M. Kitajima, *Int. J. Mod. Phys. B*, **16**, 1008 (2002).
8. B. R. Lawn, *Fracture of Brittle Solids*, Chapter 8, Cambridge Univ. Press, 1993.